Time-weighted average shear wave velocity profiles from surface wave tests through a wavelength-depth transformation.

Comina C.[1], Foti S.[2], Passeri F.[2], Socco L.V.[3]

[1]Dipartimento di Scienze della Terra, DST, Università degli studi di Torino, Torino (IT).
[2]Dipartimento di Ingegneria Strutturale, Edile e Geotecnica, DISEG, Politecnico di Torino, Torino (IT).
[3]Dipartimento di Ingegneria dell'Ambiente, del Territorio e delle Infrastrutture, DIATI, Politecnico di Torino, Torino (IT).

ABSTRACT

We investigate the possibility of obtaining time-weighted average shear wave velocity profiles through the formulation of a wavelength-depth transformation of experimental dispersion curves from surface wave tests, without a formal solution of the inverse problem. We evaluate this approach on a wide flat-file database (Polito Surface Wave Database, PSWD) of experimental dispersion curves and related shear wave velocity profiles, both from dispersion curve inversion and invasive tests. The results show that the proposed wavelength-depth transformation can be valuable for seismic site evaluations offering an estimation of time-weighted average shear wave velocity profiles very similar to a state-of-the-art inversion of the experimental dispersion curves and with similar uncertainty with respect to invasive tests. This transformation has the advantage of avoiding time-consuming inversion processes, with related uncertainty sources, and any assumption on layer parameterization and a-priori information. Moreover, in conjunction with an experimental evaluation of the fundamental frequency of the site, from independent surveys, the wavelength-depth transformation can be used to get a direct and fast estimate of the position of the engineering bedrock.

Keywords: surface waves, seismic site characterization, site classification, engineering bedrock, shear wave velocity

Corresponding author: Cesare Comina, cesare.comina@unito.it

1. INTRODUCTION

The time-weighted average shear wave velocity (*Vs,z*), sometimes referred as depth averaged shear wave velocity, is a relevant parameter to estimate the influence of near surface conditions on seismic waves propagating upwards from the bedrock (Boore, 2013). Surface wave tests are often adopted to obtain this information by the inversion of an experimentally measured dispersion curve (EDC) aimed at estimating a layered shear wave velocity (*Vs*) model (e.g. Socco et al., 2010; Foti et al., 2018; Olafsdottir et al., 2018). This model is then used to compute the *Vs,z* through the formula:

$$Vs,z = \frac{\sum_{n} h_i}{\sum_{n} \frac{h_i}{Vs_i}} \qquad (1)$$

where n is the number of layers down to the depth z, and h_i and Vs_i are the thickness and the shear wave velocity of the ith layer, respectively.

The *Vs,z* at specific depth is then used for seismic site classification and seismic site response studies. The depth of 30 m is conventionally adopted as a reference in several building codes (e.g. BSSC, 1994; CEN, 2004). The related time-weighted average shear wave velocity (i.e. $Vs,_{30}$) is also assumed as reference parameter for several applications of earthquake engineering, e.g. to develop Ground Motion Prediction Equations (GMPES). However, modern building codes (e.g. NTC, 2018; Paolucci et al., 2021) also consider specific categories for sites where the bedrock depth is less than 30 m. In this case, the whole *Vs,z* profile is required and the *Vs,h*, where *h* is the engineering bedrock depth, is assumed as reference parameter.

The main source of uncertainty in the evaluation of the layered *Vs* model from surface wave tests is due to the ill-posedness of the surface wave inverse problem. This causes severe non-uniqueness of the solution: i.e. several profiles are equivalent with respect to experimental data (Foti et al., 2009). Also, a-priori assumptions are required for the inverse problem: layer parameterization, density and Poisson ratio of the layers. The last two parameters are usually considered to have a limited influence on the dispersion curve and, consequently, on the inverse problem solution (e.g. Foti et al., 2014). However, assumptions with respect to Poisson ratio could be critical (e.g. Foti and Strobbia, 2002; Karray and Lefebvre, 2008). The layer parameterization has also a significant influence, causing uncertainty in the position of interfaces (e.g. Cox and Teague, 2016) and consequent *Vs,h* estimates. To overcome these limitations global inversion approaches have been proposed (e.g. Yamanaka and Ishida, 1996; Wathelet et al., 2004; Socco and Boiero, 2008). These approaches, being based on the computation of the EDC from a significant statistical population of profiles, allow for a robust sampling of the model parameters space. However, they are computationally intensive because of the large number of simulations to be performed (usually more than 10^5). Moreover, to overcome problems related to layer parameterization, the number of layers should be allowed to vary in the inversion process (Teague and Cox, 2016).

Reduced uncertainty is associated to the estimate of the *Vs,z* profile rather than the layered *Vs* model. Indeed, Socco et al. (2015) showed that the uncertainty due to the non-uniqueness of the solution, that affects the individual model parameters of a layered model, collapses to very low values when results are analysed in terms of *Vs,z*. Therefore, if the EDC is directly used to estimate the *Vs,z*, the solution non-uniqueness is not critical and the estimate is very robust. Several authors (e.g. Brown et al., 2000; Martin and Diehl, 2004; Comina et al., 2011; Passeri, 2019) also suggested the use of the Rayleigh wave phase velocity (*Vr*) corresponding to a specific wavelength (usually in the 36 to 42 m range) as a direct estimate of the $Vs_{,30}$. More generally the physical correlation between the wavelength of a specific harmonic of the EDC, travelling with velocity *Vr*, and the depth of the associated *Vs,z* can be exploited to directly obtain the whole *Vs,z* profile directly from the EDC, avoiding the formal solution of the inverse problem.

A similar physical correlation is adopted to obtain an approximate estimate of the *Vs* profile directly from the EDC: *Vs* values are estimated from *Vr* values by applying a correction factor and the corresponding depths are estimated as a fraction of the associated wavelength, usually between 1/2 and 1/3 (Foti et al., 2018). This approach is based on visual analysis of the trends of vertical displacements associated to Rayleigh wave propagation in a homogeneous half space. In a layered media, similar approaches were more rigorously exploited by some researchers: Aung and Leong (2015) evaluated the contribution of different layers to the *Vr* at certain wavelengths with specific weighting factors; Haney and Tsai (2015) proposed a Dix-type relationship to obtain a *Vs* depth profile directly from the EDC; Socco and Comina (2015) and Socco et al. (2017) showed that it is possible to directly transform the EDC into a *Vs,z* profile through the use of a site specific wavelength-depth transformation (W/D relationship) based on the evaluation of Rayleigh wave skin depth. This last transformation has been demonstrated to match both the *Vs,z* profiles obtained from a specific inversion of the EDCs and the ones from independent invasive tests. Moreover, the wavelength-depth transformation has demonstrated its reliability in producing 2D velocity models for waveform matching (Khosro Anjom et al., 2019) and for full waveform inversion (Teodor et al., 2021).

In this paper we extend the site-specific W/D relationship approach by using a recently published (Passeri et al., 2021) flat-file database (the Polito Surface Wave Database, PSWD) of EDCs and *Vs* profiles, both from dispersion curve inversion and invasive tests. We propose an average W/D relationship valid for different site conditions. We also evaluate the correspondence of *Vs,z* profiles computed directly by transforming the EDC with the proposed W/D relationship to the ones from a formal solution of the surface wave inverse problem and from invasive tests.

2. PSWD FLAT-FILE DATABASE AND METHODOLOGY

The PSWD flat-file Database (Passeri et al, 2021) is a gathering of EDCs and associated *Vs* profiles collected over the past 25 years at different Italian sites. For each site, a representative EDC was obtained with multi-station linear arrays (MASW), for active source tests, and 2D arrays for Ambient Vibration Analysis (AVA). Processing is based on frequency-wavenumber analysis as described in Foti et al. 2007. Alternative processing approaches (e.g. phase-shift methods or cylindrical beamforming methods) have been shown to provide very similar results, provided that the spectral resolution is adequate (Foti et al., 2018). Each EDC is associated to a best fitting *Vs* profile obtained from a two-step inversion (Passeri, 2019) with an optimised Monte Carlo inversion algorithm (Socco and Boiero 2008). This inversion strategy accounts for the influence of layer parameterization. A further strength of the adopted inversion strategy is the assumption of the Poisson ratio variability (together with number, thicknesses and shear wave velocities of the layers) in both inversion steps. Usual inversion approaches assume a-priori values for this parameter. For several sites, an independent *Vs* profile from invasive tests (mainly Down Hole tests, in few cases Cross Hole tests) is also available. Detailed description of the flat-file database together with statistical properties of test results and some inter-method comparisons are reported in Passeri et al. (2021).

For the present study, the attention is focused on a subset of 66 sites of the PSWD flat-file database. This subset was selected by considering the sites where the fundamental mode of the EDC was dominant and removing the sites with limited investigation depth (i.e. < 20 m). Due to this selection most of the considered sites show a normally dispersive behaviour and only in few sites an inversely dispersive behaviour is observed. The subset of 66 sites was then split into two groups: a first group ("Unlabelled Group") of 33 sites for which only surface wave data are available (Table 1 and Figure 1); and a second group ("Labelled Group") of 33 sites for which also an independent evaluation of the *Vs* profile from invasive tests is available (Table 2 and Figures 2 and 3).

Tables 1 and 2 reports general information about the sites: geographical location; properties of the fundamental mode EDCs in terms of available wavelength range; and the presence of independent invasive tests (available for the "Labelled Group"). For each site, literature references containing details on the surveys and on the adopted processing technique for EDC extraction can be found in Passeri et al. (2021). In these references and in Passeri et al. (2021) also further details on the geological setting of the sites, which present a great variability that picture the complexity of Italian geology, can be obtained.

Table 1 – "Unlabelled Group", for each site the geographical location and the properties of the fundamental mode EDC in terms of available wavelength range are reported.

Site information				EDC	
Site ID	**Location**	**Lat (°)**	**Long (°)**	**Wavelength Maximum [m]**	**Wavelength Minimum [m]**
1	Caselle Landi-1	45.091	9.795	70	5
2	Caselle Landi-2	45.091	9.795	47	3
3	Caselle Landi-3	45.091	9.795	61	3
4	Caselle Landi-4	45.087	9.790	102	3
5	Cesana-1	44.954	6.811	38	9
6	Cesana-2	44.953	6.809	42	3
7	Firenze-1	43.773	11.256	72	3
8	Firenze-2	43.769	11.257	45	7
9	Firenze-3	43.793	11.226	58	3
10	Gemona	46.292	13.123	73	8
11	Massa Marittima-1	43.050	10.888	49	3
12	Massa Marittima-2	43.050	10.888	49	2
13	Mathi-1	45.255	7.536	201	2
14	Mathi-2	45.255	7.536	79	3
15	Mirabello-1	44.836	11.449	35	2
16	Mirabello-2	44.836	11.449	38	2
17	Mirabello-3	44.836	11.449	42	2
18	Palmiano	42.920	13.463	55	4
19	Pontremoli-2	44.386	9.886	39	3
20	Pontremoli-3	44.374	9.881	79	6
21	Pontremoli-4	44.378	9.875	68	5
22	San Severino Marche-1	43.226	13.176	48	19
23	San Severino Marche-2	43.226	13.176	84	5
24	Settimo Torinese	45.148	7.751	90	4
25	Tarcento-4	46.216	13.224	71	3
26	Tarcento-5	46.211	13.207	72	6
27	Tarcento-8	46.214	13.219	35	4
28	Tarcento-9	46.211	13.216	77	3
29	Tarcento-10	46.212	13.219	87	6
30	Tarcento-11	46.209	13.220	89	5
31	Torre Pellice-3	44.820	7.204	46	5
32	Torre Pellice-4	44.818	7.204	55	4
33	Tarvisio	46.500	13.584	197	1

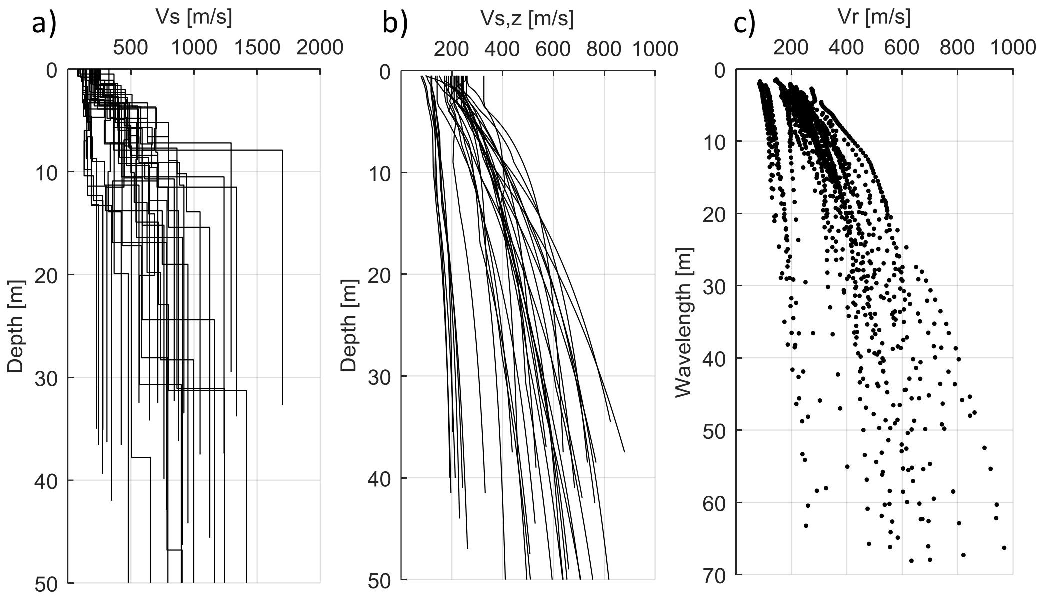

Figure 1 – "Unlabelled Group": a) best fitting shear wave velocity profiles from surface wave tests; b) time-weighted average shear wave velocity profiles from a); and c) experimental dispersion curves in the Vr-wavelength domain.

Table 2 – "Labelled Group", for each site the geographical location, the properties of the fundamental mode EDC in terms of available wavelength range and the presence of independent invasive tests are reported.

Site information				EDC		Invasive tests	
Site ID	**Location**	**Lat (°)**	**Long (°)**	**Wavelength Maximum [m]**	**Wavelength Minimum [m]**	**Down Hole**	**Cross Hole**
1	Accumoli	42.694	13.249	49	4	■	
2	Acquasanta Terme	42.771	13.414	103	4	■	
3	Castel di Lama-1	42.860	13.704	49	3	■	
4	Castel di Lama-2	42.870	13.708	83	6	■	
5	Catania	37.447	15.046	105	2	■	
6	Castelnuovo Garfagnana	44.123	10.409	73	2	■	
7	Grisciano-1	42.731	13.269	124	3	■	
8	Grisciano-2	42.730	13.268	89	3	■	
9	Grisciano-3	42.736	13.268	63	5	■	
10	Illica	42.703	13.264	55	3	■	
11	La Salle-1	45.740	7.070	427	4	■	
12	La Salle-2	45.747	7.073	351	3	■	
13	La Salle-3	45.746	7.078	444	2	■	
14	La Salle-4	45.744	7.074	347	2	■	
15	La Salle-5	45.743	7.078	123	6	■	
16	L'Aquila-1	42.328	13.409	110	1	■	
17	L'Aquila-2	42.330	13.353	92	2	■	
18	Montemonaco	42.888	13.354	43	4	■	
19	Offida	42.934	13.698	101	4	■	
20	Piazza al Serchio	44.185	10.300	31	2	■	
21	Pieve Fosciana	44.135	10.411	61	4	■	
22	Pisa	43.723	10.397	87	5		■
23	Pontremoli-1	44.371	9.881	64	8	■	
24	Roccafluvione	42.859	13.474	103	5	■	
25	Rotella	42.953	13.558	114	6	■	
26	Saluggia	45.216	8.020	75	5		■
27	Tarcento-1	46.215	13.205	49	7		■
28	Tarcento-2	46.215	13.211	43	5		■
29	Tarcento-3	46.217	13.215	47	4		■
30	Tarcento-6	46.213	13.211	59	3		■
31	Torre Pellice-1	44.817	7.220	114	6	■	
32	Torre Pellice-2	44.821	7.220	44	3	■	
33	Venarotta	42.884	13.490	41	4	■	

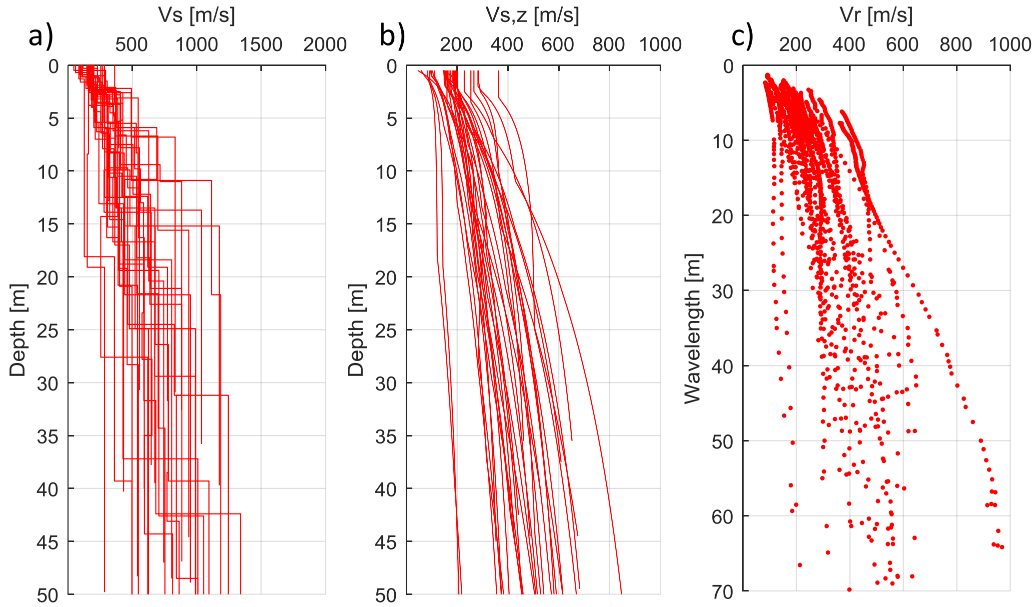

Figure 2 – "Labelled Group": a) best fitting shear wave velocity profiles from surface wave tests; b) time-weighted average shear wave velocity profiles from a); and c) experimental dispersion curves in the Vr-wavelength domain.

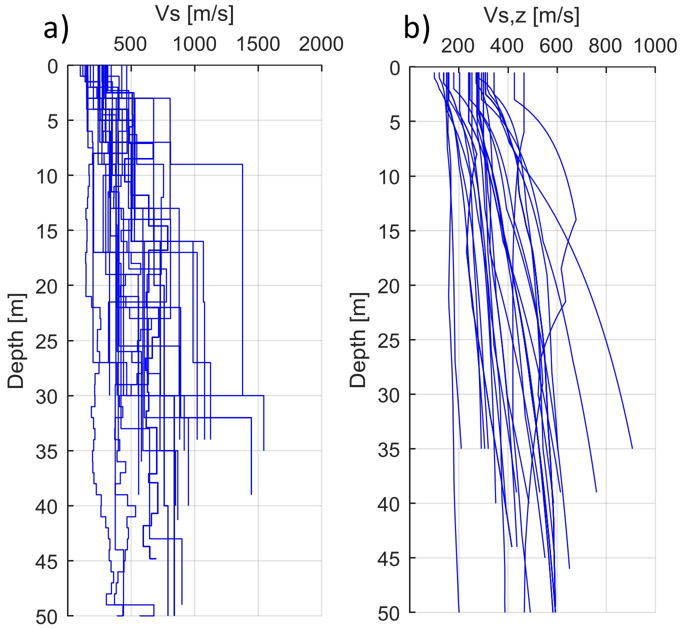

Figure 3 – "Labelled Group", for each site are reported: a) shear wave velocity profiles from invasive tests b) time-weighted average shear wave velocity profiles from a).

Figures 1, 2 and 3 show, for each site, both the layered *Vs* profiles and their corresponding *Vs,z* profiles (computed from the layered *Vs* profiles through equation 1). Figures are intended to provide an overview of the range of shear wave velocities and depths covered in the database. The fundamental mode EDCs are also represented for each site in Figures 1 and 2 in the *Vr*-wavelength domain. Both layered *Vs* and *Vs,z* profiles at each site are shown with the half-space layer extended till the maximum wavelength estimated from the EDC (see Table 1 and 2) for comparison with the corresponding EDCs in the *Vr*-wavelength domain.

For the "Unlabelled Group", each EDC and associated best fitting *Vs* profile from surface wave tests were used to compute the site-specific W/D relationships. The meaning of the site-specific W/D relationship and its computation procedure are shown in Figure 4 for one of the sites (the Torre Pellice-4 site, # 32). First the *Vs,z* profile is computed from the corresponding best fitting layered *Vs* profile (Figure 4a). Note that the value obtained for the halfspace has been extended to the necessary depth for the computation. The similitude between the *Vs,z* profile and the EDC in the *Vr*-wavelength domain (Figure 4a) is then exploited: for each *Vs,z* value, the wavelength (W) at which the phase velocity (*Vr*) of the EDC is equal to the *Vs,z* (see the arrows in Figure 4a) is searched for. In this way each wavelength value (W) is associated to the corresponding depth in the *Vs,z* profile (D). With all the W/D pairs at which *Vs,z* and *Vr* are equal a relationship is obtained (W/D relationship). This relationship represents the surface waves skin depth for increasing wavelengths and can be eventually interpolated to allow for the *Vs,z* to be computed at any depth, for the same site or for a site with similar shear wave properties.

As it can be observed from Figure 4b the shape of the W/D relationship (i.e. presence of variations in slope) is strongly related to the specific site condition and to the layering of the site, which is propagated into the shape of the EDC. For example, in Figure 4b the slope change of the EDC around 20 m depth is related to the presence of a seismic interface around that depth. Clearly, the computation of the *Vs,z* from the W/D relationship of the same site results in a perfect correspondence with the *Vs,z* computed from the best fitting *Vs* profile from the inversion, since this information is used to calibrate the W/D relationship. However, once the W/D relationship is available for a particular area of study (with similar shear wave properties) it will allow to obtain directly from other EDCs in the area the related *Vs,z* without the need for a formal solution of the inverse problem.

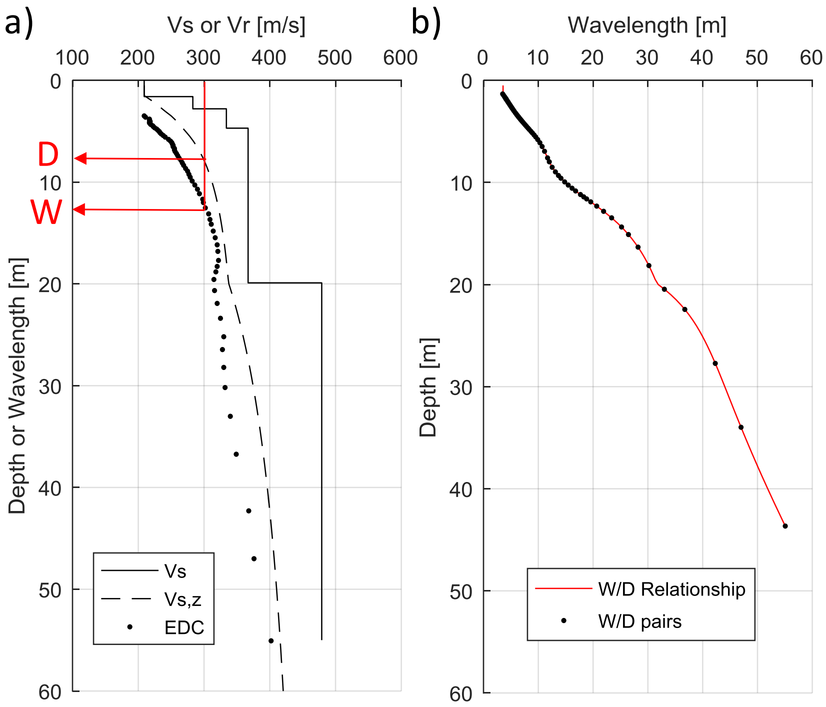

Figure 4 – "Unlabelled Group", computation of the W/D relationship for one of the sites (Torre Pellice-4 site, #32): a) in black continuous line the best fitting shear wave velocity profile from surface wave tests, in black dashed line the corresponding time-weighted average shear wave velocity profile and in black dots the experimental dispersion curve b) estimated W/D pairs for each point of the experimental dispersion curve (black dots) and piecewise polynomial regression (red line).

To extend the applicability of the W/D relationship to a wider set of subsoil conditions and to cover sites with different shear wave properties, all the EDCs and associated best fitting *Vs* profiles of the "Unlabelled Group" were analysed with the same approach described. The whole set of W/D relationships computed for the "Unlabelled Group" is plotted in Figure 5 (black dots) and an average W/D relationship is obtained computing, at each depth, the average wavelength value among the set of data and its standard deviation (both in red in Figure 5).

Very different *Vs* profiles are included in the "Unlabelled Group" (see Figure 1 a and b). Therefore, the different W/D relationships cover a wide range of variability in the shear wave properties of the formations. The differences in slope of the W/D relationships are related not only to the different shear wave velocities but also to possible differences in the Poisson ratio of the formations (Socco and Comina, 2017). Moreover, local changes in the slope of each W/D relationship are related to specific site layering (see the example in Figure 4).

The average W/D relationship therefore represents different shear wave velocities, Poisson ratios and formation layering among the various sites included in the "Unlabelled Group". These differences are more relevant for increasing depths (particularly in terms of shear wave properties) and this reflects the fact that the standard deviation error bars of the average W/D relationship also increase for increasing depths.

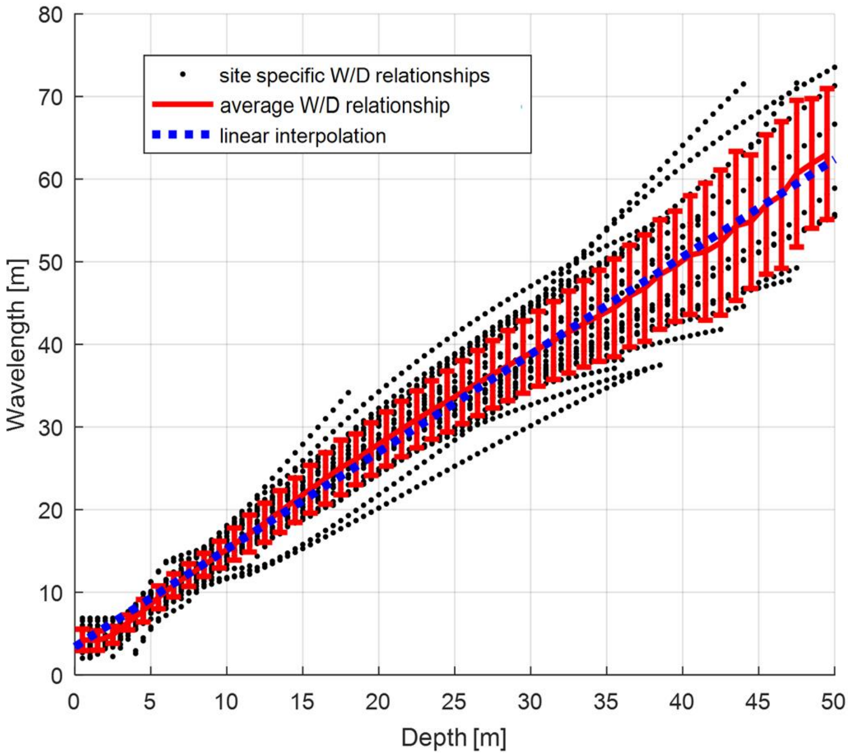

Figure 5 – "Unlabelled Group", computation of the average W/D relationship: site specific W/D relationships for each best fitting shear wave velocity profile and corresponding experimental dispersion curve (black dots) and average W/D relationship (red line and error bars) together with its linear interpolation (blue dashed line).

A linear interpolation is an acceptable approximation of the average W/D relationship (see Figure 5), as confirmed by the adjusted R-square value of 0.998. This approach has also the advantage of a compact formulation and ease of use. Therefore, the proposed formulation of the linear wavelength-depth transformation, used in the following is:

$$z_i = 0.84 \cdot w_i - 2.84 \qquad (2)$$

were w_i are the wavelengths of each EDC point and z_i their corresponding depths. With this formulation it is possible to transform any available EDC in its corresponding *Vs,z* profile without performing the inversion process and without further assumptions.

This transformation is applied to each EDC of both the "Unlabelled" and "Labelled" Groups to evaluate its performance for the direct estimate of the *Vs,z* profiles. Results are compared to the ones obtained both from EDC inversion and invasive tests, available for the "Labelled Group". This comparison is performed, at each depth, in terms of normalized differences (*ND(z)*) with the formula:

$$ND(z) = \frac{Vs,z^{WD} - Vs,z^{SWI,I}}{Vs,z^{SWI,I}} \qquad (3)$$

where Vs,z^{WD} is the *Vs,z* value obtained from the linear wavelength-depth transformation and $Vs,z^{SWI,I}$ are the *Vs,z* values obtained from surface wave tests (SWI) or from invasive tests (I), both considered as benchmarks.

Note that for the "Labelled Group" the application of the wavelength-depth transformation gives a blind prediction. Therefore, the *ND(z)* values obtained for the "Labelled Group" provide a valuable judgement on the applicability of the transformation (equation 2) to any site.

3. RESULTS

In Figure 6 the results obtained from the application of the transformation (equation 2) to the "Unlabelled Group" are reported. The normalized differences in *Vs,z* profiles from the application of the transformation and from the inversion are shown in Figure 6c.

On average, the normalized differences are greater in the shallow portion of the profile (i.e. within the first 5 m) and decrease for increasing depths (except for few isolated cases). This effect is also related to the poor fitting of the linear interpolation with the average W/D relationship at shallow depths (see Figure 5). From the depth of 5 m, the normalized differences remain, for most of the profiles, within a ± 6% difference (see the standard deviation lines in Figure 6c). This is an indication that the proposed approach provides similar accuracy if compared to the formal inverse problem solution. Laborious inversion step and any assumption with respect to layer parameterization and a-priori information are avoided.

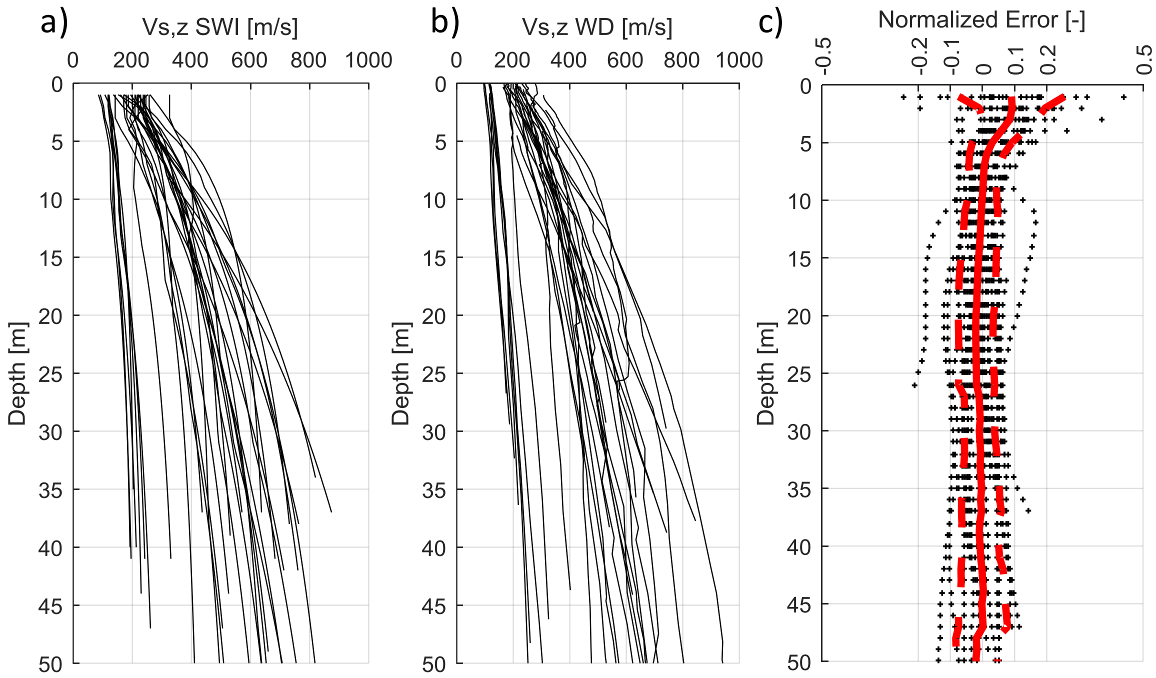

Figure 6 – "Unlabbelled Group", comparison of Vs,z profiles (in black) from a) best fitting shear wave velocity profiles from surface wave tests, b) the application of the linear wavelength-depth transformation to each site EDC and c) their normalized differences (black crosses) with evidence of average error (red continuous line) and standard deviation (red dashed line).

In Figure 7 and 8 the results obtained from the application of the transformation to the "Labelled Group" are reported. The normalized differences between the *Vs,z* profiles obtained from the transformation and those obtained from the inversion (Figure 7c) are of the same order (± 6% difference) of the ones retrieved on the "Unlabelled Group", for depths below 5 m. This is an indication that the proposed transformation provides similar accuracy also for data not contained in the dataset from which it was estimated. Only a slight average underestimation (-4 %) of the *Vs,z* profiles can be observed in the 20 to 40 m depth range. This effect may be related to the average lower velocities (around 60 m/s) of the "Labelled Group" with respect to the "Unlabelled Group" (see Figure 1a and 2a). Conversely, the normalized differences between the *Vs,z* profiles obtained from the transformation and from invasive tests (Figure 8c) is greater and a general tendency of the transformation to underestimate the velocity is observed (average normalized differences around -15 %). It must be however underlined that the observed differences with respect to invasive tests is very similar to the ones observed between the same invasive tests and the results of EDC inversion (see Figure 9 in Passeri et al., 2021).

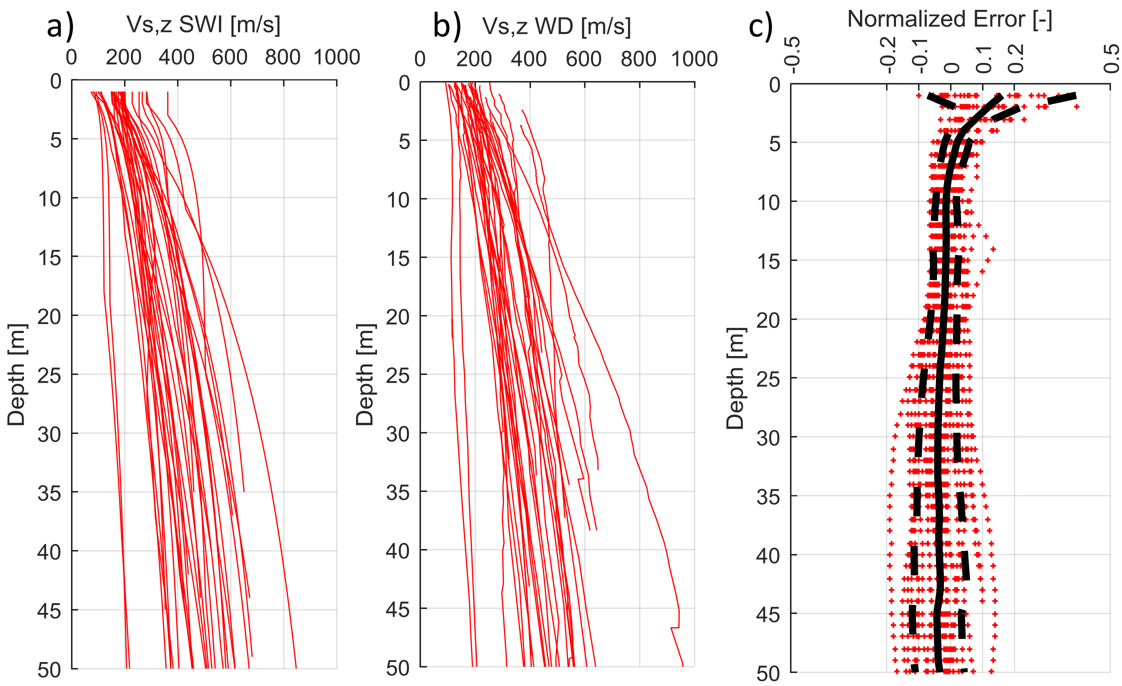

Figure 7 – "Labelled Group", comparison of Vs,z profiles (in red) from a) best fitting shear wave velocity profiles from surface wave tests, b) the application of the linear wavelength-depth transformation to each site EDC and c) their normalized differences (red crosses) with evidence of average error (black continuous line) and standard deviation (black dashed line).

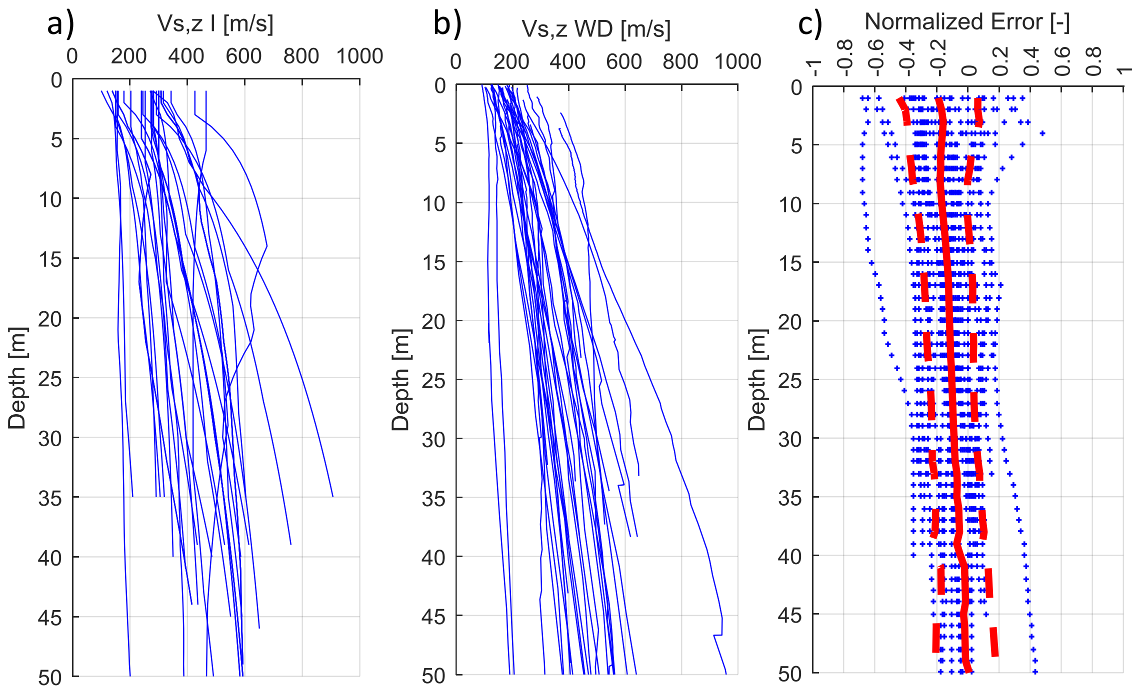

Figure 8 – "Labelled Group", comparison of Vs,z profiles (in blue) from a) invasive tests, b) the application of the linear wavelength-depth transformation to each site EDC and c) their normalized differences (blue crosses) with evidence of average error (red continuous line) and standard deviation (red dashed line).

3.1 Use for seismic site classification

The estimation of the *Vs,z* through the proposed linear wavelength-depth transformation can be adopted to efficiently compute parameters commonly used for seismic site classification (e.g. $Vs_{,30}$ or *Vs,h*). The reliability of the transformation is evaluated in the following with reference to the Italian building code (NTC, 2018), which adopts *Vs,h* as classification parameter (i.e. *Vs,z* till the depth *h* of the engineering bedrock). A similar approach has been also recently proposed for the new generation of Eurocodes (Paolucci et al., 2021). For these computations the depth *h* was assumed equal to the depth of the conventional engineering bedrock ($Vs \geq 800$ m/s), if this velocity was reached within 30 m. Otherwise the depth *h* value was assumed equal to 30 m, as required by the code. Results of the comparison of the *Vs,h* values obtained from the *Vs,z* profiles through the transformation or from surface wave inversion and invasive tests are reported in Figures 9 and 10.

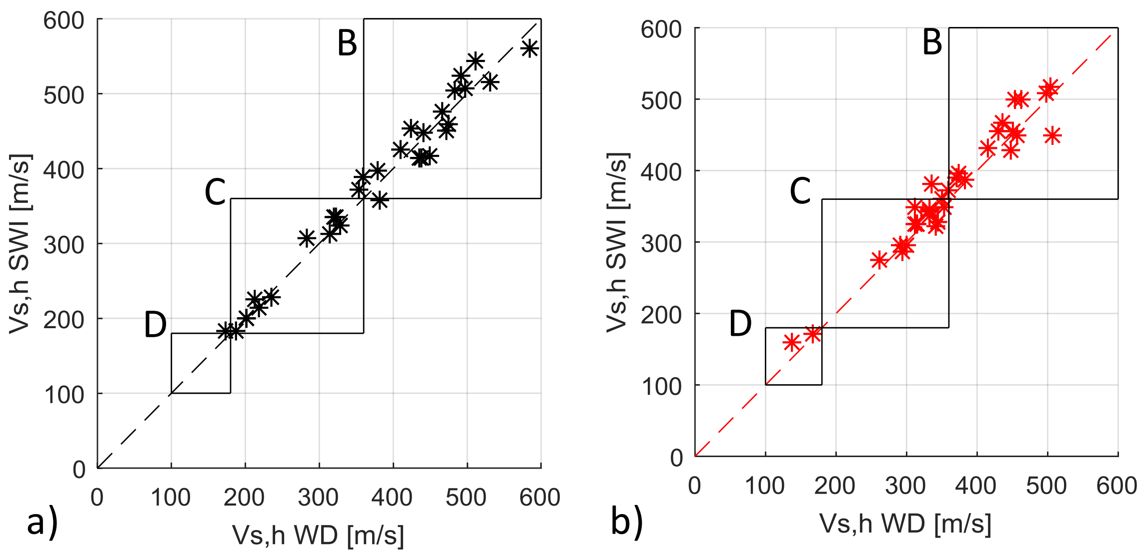

Figure 9 –Comparison of Vs,h values from the application of the linear wavelength-depth transformation to each site EDC and from best fitting shear wave velocity profiles from surface wave tests in a) the "Ulabelled Group" and b) the "Labelled Group"; the 1:1 line and borders of the seismic soil classes from Italian normative (NTC, 2018) are also evidenced.

From these comparisons it can be observed that, with respect to surface wave inversion, only for a couple of sites (one for the "Unlabelled Group" and one for the "Labelled Group" respectively) the proposed approach fails in identifying the same seismic soil class (Figure 9). For most of the sites, the same soil class is obtained also for sites close to the boundaries between two soil classes.

Conversely a few sites (seven) failed to be identified in the same seismic soil class if comparing the results from the application of the transformation and from invasive tests (Figure 10). The observed discrepancies in the evaluations is however very similar to the differences observed between the same invasive tests and the results of a formal EDC inversion (see Figure 10 in Passeri et al., 2021). Therefore, this result is not an index of reduced reliability in the application of the linear wavelength-depth transformation but of the general difference between surface waves and invasive tests. In general terms, it is a good practice to classify the sites in the lower class whenever the estimated values of *Vs,h* are close to the boundary between two classes, in order to account for uncertainties in seismic tests.

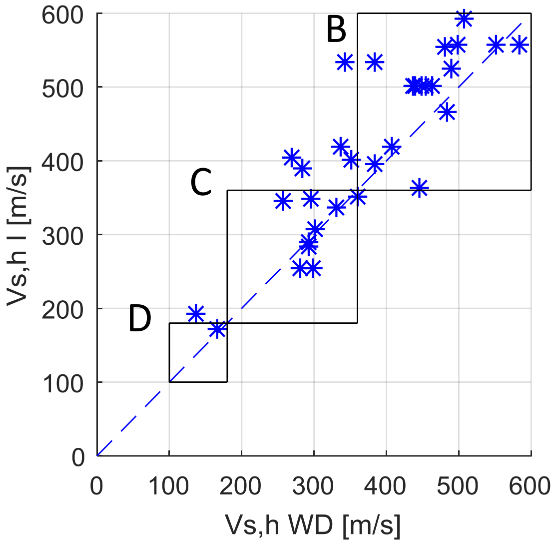

Figure 10 – Comparison of Vs,h values from the application of the linear wavelength-depth transformation to each site EDC and from invasive tests in the "Labelled Group"; the 1:1 line and borders of the seismic soil classes from Italian normative (NTC, 2018) are also evidenced.

3.2 Use for bedrock depth estimation

As shown in the previous section, the depth of the engineering bedrock *h* is required to compute the *Vs,h* (i.e. *Vs,z* till the depth *h*). This information can be obtained using the proposed linear wavelength-depth transformation when an experimental evaluation of the site fundamental frequency (f_0) is available from independent tests (e.g. from HVSR Horizontal-to-Vertical Spectral Ratio, see SESAME, 2004). Often the analysis of ambient vibration (passive surface wave test) is carried out using 3C receivers and the data can be used also for HVSR analysis.

The link between the site fundamental frequency f_0 and the depth of the engineering bedrock *h* can be expressed through the value of *Vs,h* as:

$$fo = \frac{Vs, h}{4 \cdot h}. \qquad (4)$$

On the other side, the *Vs,z* profile from the linear wavelength-depth transformation can be converted to a relationship expressing different possible values of fundamental frequencies *f* at any depth *z* through the same equation:

$$f(z) = \frac{Vs,z}{4 \cdot z}, \qquad (5)$$

and used to evaluate the specific depth *h* at which the *f* value equals the site measured f_0. This will allow to contemporary estimate the *Vs,h* and the bedrock depth *h*.

An example is provided in the following for the Mirandola test site, which is not part of the PSWD (Passeri et al., 2019). This test site has been investigated in detail in the past with several independent surveys (Garofalo et al., 2016a and 2016b). Specifically, two drillings, 126 m deep and at a distance of about 6 meters from each other, were available for Cross Hole measurements and both active and passive seismic data were collected with arrays close to the boreholes. Several comparisons between surface wave tests and invasive methods were performed to reach a consistent subsurface characterization.

Site investigations identified a deep engineering bedrock (at the depth of around 117 m in the boreholes), consisting of consolidated mudstones with interbedded sands, referring to marine and transitional deposits of the middle Pliocene. Above this bedrock alluvial deposits with alternating sequences of silty-clayey layers and sandy horizons are present. In Figure 11a the *Vs* profiles form Cross Hole tests (CH) and from the inversion of one of the wider frequency band EDC at the site (SWI) are reported.

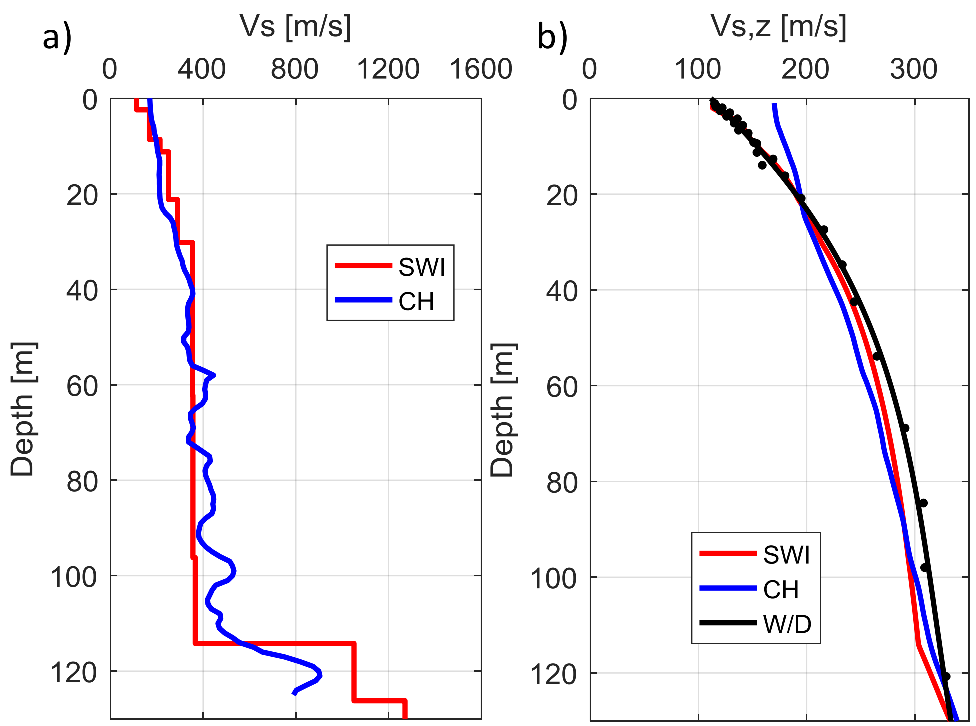

Figure 11 – Mirandola test site, comparison of a) Vs and b) Vs,z profiles from: invasive tests (CH in blue) and inversion of surface wave tests (SWI in red); in b) also the application of the linear wavelength-depth transformation to the considered EDC is reported (W/D in black continuous line and dots).

Also, several independent estimates of the fundamental frequency of the deposit (f_0) with the HVSR method are available (Passeri et al., 2019). A clear resonance peak is found around 0.72 Hz, with very limited spatial variability over the site. Therefore, no significant lateral variations are present at the site (horizontal layering), as expected in that geological environment.

In Figure 11b results from the application of the transformation (equation 2) to the same EDC used for the inversion are compared in terms *Vs,z* to the CH and SWI results. An overestimation of the velocity from CH test is noted, in the shallower portion of the profile, with respect to both SWI and the transformation. These differences reduce however with depth. Conversely with the general tendency of underestimating the *Vs,z* profile from the transformation with respect to invasive tests, for this specific test site both SWI and the transformation provide a moderate overestimation in the 20 to 100 m depth range (indeed limited to at most 20 m/s).

The *f* conversion of the linear wavelength-depth transformation (equation 5) was then performed to obtain the *f* vs. *z* curve (Figure 12). Considering the site measured f_0, the bedrock *h* (see the arrows in Figure 12) and corresponding *Vs,h* can be obtained. Table 3 reports the estimated values against the results from CH and SWI.

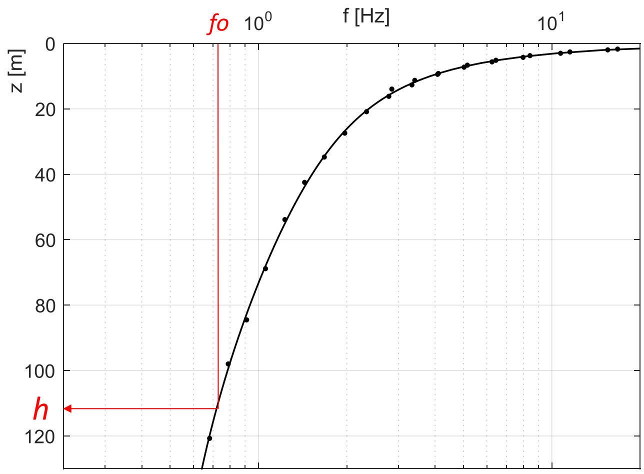

Figure 12 – Mirandola test site, *f* vs. *z* relation from the linear wavelength-depth transformation and direct estimation of the bedrock depth.

Table 3 – Mirandola test site, comparison of depth to the bedrock (h) and time-weighted average velocity to this depth (Vs,h) from invasive tests (CH), inversion of surface wave tests (SWI) and the application of the linear wavelength-depth transformation (W/D).

	h [m]	Vs,h [m/s]
from W/D	115.6	324
from SWI	114.2	302
from CH	117	322

4. DISCUSSION

The results reported in the paper demonstrate the applicability of the linear wavelength-depth transformation as a fast tool for the interpretation of surface wave data that allow to directly obtain the *Vs,z* profile without a formal solution of the inverse problem. A similar approach was proposed in the past to estimate the $Vs_{,30}$ with empirical correlations with the Rayleigh wave phase velocity at a specific wavelength (e.g. Brown et al., 2000; Martin and Diehl, 2004; Comina et al., 2011; Passeri, 2019). Consistently with these studies, the proposed transformation provides a reference wavelength for $Vs_{,30}$ in the 34 to 44 m range (Figure 5). Moreover, the general trend of the linear wavelength-depth transformation is in line with previous studies (e.g. Tsitos et al. 2004; Pelekis and Athanasopoulos, 2011; Pan et al., 2013) that investigate the surface waves skin depth, through the quantification of specific w/z ratios, by looking at the surface waves displacement profiles with depth for different wavelengths.

In comparison with other works that exploite the surface waves skin depth concept (e.g. Aung and Leong, 2015; Haney and Tsai, 2015), the linear wavelength-depth transformation has the main advantage of not requiring any minimization step, as it directly provides the whole *Vs,z* profile through a simple data transform.

The linear wavelength-depth transformation was shown to perform well for 5m depth onwards. Given the purpose of the method to obtain the *Vs,z* for seismic site classification, this cannot be considered an issue as typically *Vs,z* is required at depths higher than 5 m. For increasing depths the transformation was shown to provide *Vs,z* profiles within a ± 6% difference with the ones from a state of the art inversion of the same data (Figures 6c and 7c). It was also shown to provide a very similar soil class identification (Figure 9).

Conversely, an increased difference was noted between the *Vs,z* profiles from the application of the transformation and from invasive tests (Figure 8c). An average -15 % underestimation of velocity was observed. It was also shown that the seismic soil class identification through the transformation is, for some of the sites, underestimated with respect to invasive tests (Figure 10). This underestimation is, however, related to the general difference between surface waves and invasive tests and it is not a specific pitfall of the transformation. In this respect, it must be underlined that also invasive tests are subjected to a non-negligible uncertainty, particularly for shallow depths. Near-surface effects are recognized for invasive methods which tend to have measuring errors for the few uppermost meters (e.g. Moss, 2008). Indeed, the normalized differences from the application of the transformation and from invasive tests (Figure 8c) are larger near the surface (average normalized differences around -20 %) and decrease with depth. The constant negative difference among the results may be related to the strain hardening due to grouting operations which result in an overestimation of the velocity in invasive tests. Moreover, also the different volumes investigated by the two methodologies could play a role in this difference.

The proposed formulation of the linear wavelength-depth transformation (equation 2) is based on the data from Italian sites contained in the PSWD. Therefore, its applicability in other area of study should be verified. Also, alternative formulations to the one proposed may be chosen adopting a regression line without an intercept (as in Socco and Comina, 2015) or a more elaborated piece-wise polynomial interpolation (as in Socco et al., 2017). However, the effect of removing the intercept in the regression or adopting a pice-wise interpolation would be mainly relevant at shallow depths with a reduced influence on the seismic site classification.

Nevertheless, the wide variability of *Vs,z* profiles contained in the PSWD (with *Vs,h* values ranging from 100 to 600 m/s) suggests a wide range of applicability. It was also shown that the application of the proposed transformation to a different dataset for which it was formulated (i.e. "Unlabelled" and "Labelled" groups) allow to obtain similar results with respect to EDC inversion if the average difference in the velocity distribution of the two datasets is around 60 m/s. To evaluate more specifically the performances of the proposed approach in different contexts, the development of site specific W/D relationships and related wavelength-depth transformations could be foreseen (i.e. calibration of the coefficient of equation 2), adopting the same approach of this paper. This can be attempted in sites with a significantly different velocity distribution.

These site specific W/D relationships would also have a stronger link with formation layering and shear wave velocity properties and will allow an even increased correspondence with the inversion results. Socco et al. (2017) showed that a W/D relationship calibrated on one single *Vs* model and corresponding EDC allowed to estimate *Vs,z* profiles from other different EDCs in the same dataset with uncertainty of the order of 10% for synthetic data simulating a site condition with strong velocity variations and approximately 5% for field data in a site with smooth velocity variations. They also confirmed the applicability of the proposed approach in inversely dispersive sites: i.e. containing a low-velocity layer embedded in higher velocity layers. With the use of more site specific W/D relationships also a direct computation of the layered shear wave velocity model would be possible (Khosro Anjom et al., 2019). Moreover, the slope of the site specific W/D relationship has been observed to have a strong link with the Poisson ratio of the formation (Socco and Comina, 2017) allowing the compressional wave velocities (*Vp*) to be estimated from the same EDC as shown in Comina et al. (2020).

5. CONCLUSIONS

A linear wavelength-depth transformation was proposed in the paper for the direct estimate of the time-weighted average shear wave velocity (*Vs,z*) from the experimental dispersion curve. We showed that the obtained *Vs,z* profiles stand within a ± 6% difference with the ones obtained with a state-of-the-art inversion of the same experimental dataset and have similar uncertainty with respect to invasive tests. Moreover, in conjunction with an experimental evaluation of the fundamental frequency of the site from other tests, the linear wavelength-depth transformation can be used to get a direct and fast estimate of the position of the engineering bedrock.

The proposed wavelength-depth transformation can be therefore considered as a valuable and efficient tool for seismic site classification. It has indeed has several advantages: i) being a data transformation approach it does not require time-consuming inversion processes; ii) it does not require any assumption with respect to the layer parameterization or does not require multiple parameterizations to be computed with a time-consuming global inversion approach; iii) it does not make any a-priori assumption with respect to density and Poisson ratio.

DATA AVAILABILITY

The data underlying this article are available in open access as an electronic supplement of the publication: Passeri F., Comina C., Foti S., Socco L.V. (2021) The Polito Surface Wave flat‑file Database (PSWD): statistical properties of test results and some inter‑method comparisons, Bulletin of Earthquake Engineering, 19, pages 2343–2370. https://doi.org/10.1007/s10518-021-01069-1.

REFERENCES

1. Aung, A. M. W., and E. C. Leong, 2015, Application of weighted average velocity (WAVe) method to determine VS;30: Soils and Foundations, 55, 548–558.
2. Boore, D. M., 2013, The uses and limitations of the square-root-impedance method for computing site amplification, Bulletin of the Seismological Society of America: 103(4), 2356-2368
3. Brown, L., Diehl, J. G., and Nigbor, R. L. A simplified procedure to measure average shear-wave velocity to a depth of 30 meters (VS30). Proceedings of 12th world conference on earthquake engineering, 2000. 1-8.
4. BSSC (1994) "NEHRP Recommended provisions for the development of seismic regulations for new buildings, part I: Provisions", Building Seismic Safety Council, Federal Emergency Management Agency, Washington D.C.
5. CEN (2004) "EN 1998-1 Eurocode 8: Design of structures for earthquake resistance", Brussels.
6. Comina, C., Foti, S., Boiero, D., and Socco, L., 2011. Reliability of VS, 30 evaluation from surface-wave tests, Journal of geotechnical and geoenvironmental engineering 137, 579-586.
7. Comina, C., Vagnon, F., Arato, A., Antonietti, A. (2020) Effective Vs and Vp characterization from Surface Waves streamer data along river embankments, Journal of Applied Geophysics, 183, art. no. 104221.
8. Cox, B. R. and Teague, D. P., 2016, Layering ratios: a systematic approach to the inversion of surface wave data in the absence of a priori information, Geophys. J. Int. (2016) 207, 422–438.
9. Foti, S., and C. Strobbia, 2002, Some notes on model parameters for surface wave data inversion: Symposium on the Application of Geophysics to Engineering and Environmental Problems SAGEEP, SEI6.
10. Foti S., Comina C. and Boiero, D., 2007. Reliability of combined active and passive surface wave methods, Rivista Italiana di Geotecnica, anno XLI, n°2, pp 39 - 47, Patron Editore, ISSN 0577-1405.
11. Foti, S., Comina, C., Boiero, D., and Socco L. V., 2009, Non-uniqueness in surface-wave inversion and consequences on seismic site response analyses, Soil dynamics and Earthquake Engineering: 29(6), 982-993.
12. Foti, S., Hollender, F., Garofalo, F., Albarello, D., Asten, M., Bard, P.-Y., Comina, C., Cornou, C., Cox, B., and Di Giulio, G., Forbriger T., Hayashi K., Lunedei E., Martin A., Mercerat D., Ohrnberger M., Poggi V., Renalier F., Sicilia D., Socco L.V., 2018. Guidelines for the good practice of surface wave analysis: a product of the InterPACIFIC project, Bulletin of Earthquake Engineering 16, 2367-2420.
13. Foti, S., Lai, C. G., Rix, G. J., and Strobbia, C. 2014. Surface wave methods for near-surface site characterization, CRC Press.
14. Garofalo F, Foti S, Hollender F, Bard P, Cornou C, Cox B, Ohrnberger M, Sicilia D, Asten M, Di Giulio G., 2016b, InterPACIFIC project: comparison of invasive and noninvasive methods for seismic site characterization. Part I: intra-comparison of surface wave methods. Soil Dynam Earthq Eng.
15. Garofalo F, Foti S, Hollender F, Bard P, Cornou C, Cox B, Dechamp A, Ohrnberger M, Perron V, Sicilia D., 2016b, InterPACIFIC project: comparison of invasive and non-invasive methods for seismic site characterization. Part II: intercomparison between surface-wave and borehole methods. Soil Dynam Earthq Eng.
16. Haney, M. M., and V. C. Tsai, 2015, Non perturbational surface-wave inversion: A Dix-type relation for surface waves: Geophysics, 80, no. 6, EN167–EN177.
17. Karray, M., and G. Lefebvre, 2008, Significance and evaluation of Poisson's ratio: Canadian Geotechnical Journal, 45, 624–635.
18. Khosro Anjom, F., D. Teodor, C. Comina, R. Brossier, J. Virieux, and L. V. Socco, 2019, Full waveform matching of Vp and Vs models from surface waves, Geophysical Journal International, 218, 1873-1891.
19. Martin, A. J., and Diehl, J. G. Practical experience using a simplified procedure to measure average shear-wave velocity to a depth of 30 meters (VS30). 13th World Conf. on Earthquake Engineering, 2004. International Association for Earthquake Engineering Tokyo.
20. Moss, R. E. S., 2008. Quantifying measurement uncertainty of thirty-meter shear-wave velocity, Bulletin of the Seismological Society of America 98, 1399-1411.
21. NTC, 2018. Norme Tecniche per le Costruzioni Consiglio Superiore dei Lavori Pubblici, Ministero per le Infrastrutture e dei Trasporti.

22. Olafsdottir, E.A., Erlingsson, S., and Bessason, B. (2018). Tool for analysis of multichannel analysis of surface waves (MASW) field data and evaluation of shear wave velocity profiles of soils. Canadian Geotechnical Journal.
23. Pan, Y., J. Xia, L. Gaoa, C. Shen, and C. Zeng, 2013, Calculation of Rayleigh-wave phase velocities due to models with a high-velocity surface layer: Journal of Applied Geophysics, 96, 1–6.
24. Paolucci, R., Aimar, M., Ciancimino, A. et al. Checking the site categorization criteria and amplification factors of the 2021 draft of Eurocode 8 Part 1–1. Bull Earthquake Eng (2021). https://doi.org/10.1007/s10518-021-01118-9.
25. Passeri, F. 2019. Development of an advanced geostatistical model for shear wave velocity profiles to manage uncertainties and variabilities in Ground Response Analyses Ph.D. dissertation, Politecnico di Torino.
26. Passeri F, Foti S, Rodriguez-Marek A 2020. A new geostatistical model for the management of uncertainties in shear wave velocity proiles, Soil Dynamics and Earthquake Engineering, 136, art. no. 106247.
27. Passeri F., Comina C., Foti S., Socco L.v. (2021) The Polito Surface Wave flat‑file Database (PSWD): statistical properties of test results and some inter‑method comparisons, Bulletin of Earthquake Engineering, 19, pages2343–2370.
28. Pelekis, P. C., and G. A. Athanasopoulos, 2011, An overview of surface wave methods and a reliability study of a simplified inversion technique: Soil Dynamics and Earthquake Engineering, 31, 1654–1668.
29. SESAME (2004). Guidelines for the implementation of the H/V spectral ratio technique on ambient vibration: measurements processing and interpretation, http:// sesame.geopsy.org / Papers / HV_User_Guidelines.pdf
30. Socco, L.V. and Boiero D. (2008) "Improved Monte Carlo inversion of surface wave data" Geophysical Prospecting, 56, 357-371.
31. Socco, L.V., S. Foti, D. Boiero, 2010, Surface wave analysis for building near surface velocity models: established approaches and new perspectives: Geophysics, 75, 5, 75A83 – 75A102.
32. Socco, L.V., Mabyalaht, G., Comina, C. (2015) Robust static estimation from surface wave data, SEG Technical Program Expanded Abstracts, 34, pp. 5222-5227.
33. Socco, L.V., Comina, C. (2015) Approximate direct estimate of S-wave velocity model from surface wave dispersion curves, Near Surface Geoscience 2015 - 21st European Meeting of Environmental and Engineering Geophysics, pp. 251-255.
34. Socco, L. V., Comina, C., and Khosro Anjom, F., 2017. Time-average velocity estimation through surface-wave analysis: Part 1—S-wave velocity, Geophysics 82, U49-U59.
35. Socco, L.V. and Comina, C., 2017. Time-average velocity estimation through surface-wave analysis: Part 2—P-wave velocity, Geophysics, 82(3), U61–U73.
36. Teague, D. P., and Cox, B. R., 2016. Site response implications associated with using non-unique vs profiles from surface wave inversion in comparison with other commonly used methods of accounting for vs uncertainty, Soil Dynamics and Earthquake Engineering 91, 87-103.
37. Teodor D., Comina C., Khosro Anjom F., Socco L.V., Brossier R. and Virieux J., 2020, Challenges in shallow targets reconstruction by 3D elastic full-waveform inversion – Which initial model?, Geophysics, Volume 86, Issue 4, Pages 1 - 14.
38. Tsitos AC, Vlachakis VS, Pelekis PC, Athanasopoulos GA. Numerical simulation of the spectral analysis of surface waves (SASW) method—parametric analyses. In: Proceedings of the 11th international conference on soil dynamics & earthquake engineering (11th ICSDEE) and 3rd international conference on earthquake geotechnical engineering (3rd ICEGE). University of California, vol. 1. Stallion Press; January 2004. p. 538–45.
39. Wathelet, M., Jongmans, D. & Ohrnberger, M., 2004. Surfacewave inversion using a direct search algorithm and its application to ambient vibration measurements, Near Surf. Geophys., 2, 211–221.
40. Yamanaka, H. & Ishida, H., 1996. Application of generic algorithms to an inversion of surface-wave dispersion data, Bull. Earthq. Eng., 86, 436– 444.